

## Supporting Information

### Qualitative Rationalization of Crystal Growth Morphology of Benzoic Acid Controlled by Solvent

Zuozhong Liang<sup>a</sup>, Jian-Feng Chen<sup>a</sup>, Ying Ma<sup>a</sup>, Wei Wang<sup>a</sup>, Xianglong Han<sup>a</sup>, Chunyu Xue<sup>\*b</sup>,  
Hong Zhao<sup>\*a</sup>

<sup>a</sup> State Key Laboratory of Organic-Inorganic Composites, Beijing University of Chemical  
Technology, Beijing 100029, PR China

<sup>b</sup> Biomass Energy and Environmental Engineering Research Center, Beijing University of  
Chemical Technology, Beijing 100029, PR China

\*Contact information:

Chunyu Xue

E-mail: cyxue2011@gmail.com;

Tel./fax: +86 1064442375;

Hong Zhao

E-mail: zhaohong.buct@gmail.com;

Tel.: +86 1064433134; fax: +86 1064434784.

## 1. Simulation details

The modeling of benzoic acid (BA) crystal growth morphology was carried out using the Material Studio 6.0 from ACCELRYYS.<sup>1</sup> The crystal unit cell of BA (CSD Refcode BENZAC02) is a monoclinic lattice with space group  $P2_1/c$ ,  $Z=4$ , and cell parameters  $a=5.50$ ,  $b=5.128$ ,  $c=21.950$ ,  $\alpha=90^\circ$ ,  $\beta=97.370^\circ$ ,  $\gamma=90^\circ$ .

The initial step of crystal habit prediction is the computation of ideal morphology by means of AE method with the PCFF force field.<sup>2</sup> The resulting crystal habit provides eight morphologically important (MI) facets considered in subsequent molecular dynamics (MD) simulations. In preparation of simulations on the growth process, these facets are cleaved to a fractional depth of  $3 \times d_{hkl}$ . Then a supercell, so-called crystal layer, is created and fitted with a 80-Å vacuum slab. Subsequently, the crystal layer is optimized by MD simulation and the result potential energy is defined as  $E_{\text{crystal}}$ .

The second step is constructing the solvent mixture layer, which contains a random arrangement of solvent molecule and solute molecule with different molar ratios. The size parameters of solvent mixture layer should be agreement with the corresponding crystal layer. And molecules in this layer are positioned randomly and could move freely under the specific conditions, such as temperature, density, and amount of molecules. Then the minimization is conducted at enough iteration steps to equilibrate the layer. The subsequent MD simulation is performed using the isothermal-isovolumetric ensemble (NVT—constant number of particles  $N$ , constant volume  $V$ , and constant temperature  $T$ ) 50 ps with a time step of 1 fs using the Velocity Scaling thermostat as the temperature control algorithm with  $\Delta T=10$  K. For potential-energy calculations, the Ewald summation method is used to calculate both van der Waals and Coulomb interactions, with a calculation accuracy of  $0.001 \text{ kcal}\cdot\text{mol}^{-1}$  and a spline cutoff distance of 12.5 Å. The equilibrium potential energy is expressed as  $E_{\text{solution}}$ .

Finally, the interfacial layer, called modeling box, is constructed. The modeling box contains the crystal layer, the solvent mixture layer and a vacuum slab (50 Å) to eliminate the effect of boundaries. Before the simulation, atoms of the crystal surface

in this interfacial layered system are fixed in their Cartesian position. The subsequent MD simulation of the modeling box is conducted using canonical ensemble NVT at a time step of 1 fs for 50 ps and followed a minimization of 20,000 iterations using the Newton algorithm to equilibration and the lowest energy is named as  $E_{\text{box}}$ .

Eventually, the modified AE  $E_{\text{mod}}$  is calculated to simulate the growth of BA crystal and generate predicted crystal habit.

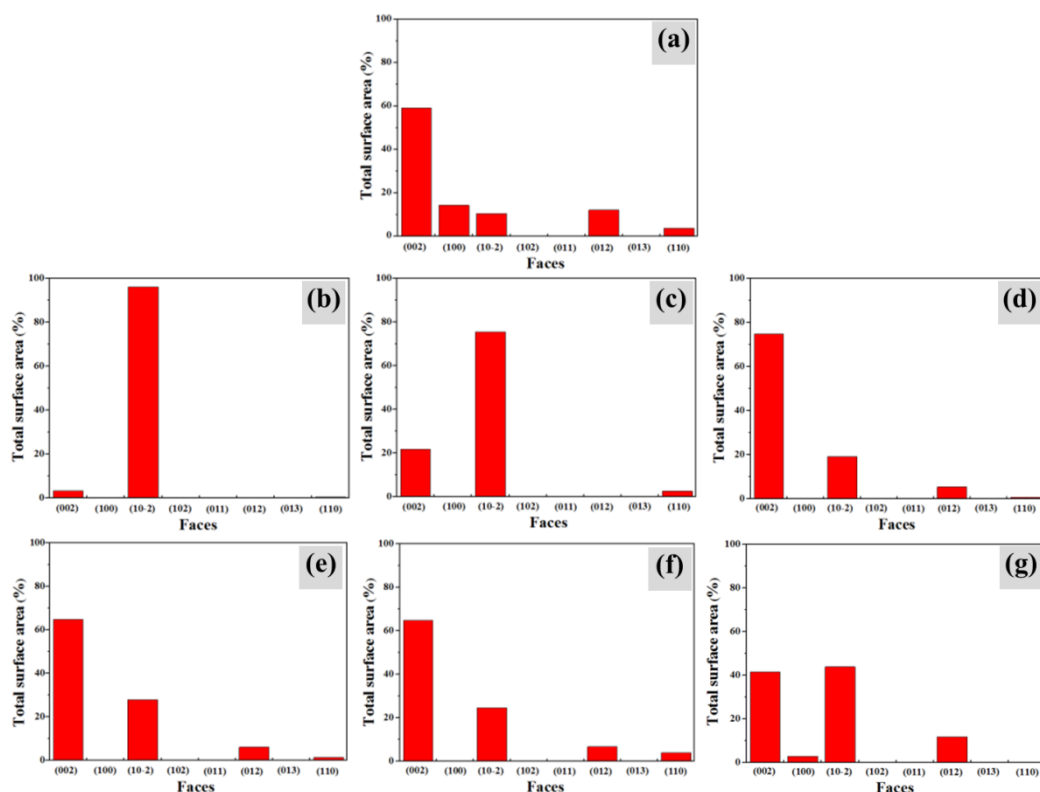
## 2. Solvent properties

Table S1 Properties of different solvents (Measured in 25°C)

Solvents	n-hexane	n-heptane	toluene	isopropanol	acetone	acetonitrile
Polarity / $P_1$	0	0.2	2.4	3.9	5.4	6.2
Solubility(kg m <sup>-3</sup> )/ $S$	8	9	50	100	300	534
Molecule weight/ $M$	86.17	100.21	92.13	60.09	58.08	41.05
Permittivity/ $P_2$	1.890	1.924	2.24	18.3	20.70	37.5
Evaporation rate/ $E$	1000	386	195	205	1120	630
Vapor pressure(kPa)/ $V$	20	6.2	3.8	5.8	30.56	12.6

\*The value of evaporation rate based on the suppose n-butyl acetate  $E=100$ .

## 3. Total surface area



**Fig. S1** Total surface area of predicted BA crystal habits in vacuum (a) and different solvents (b-n-hexane, c-n-heptane, d-toluene, e-isopropanol, f-acetone, g-acetonitrile).

**Fig. S1** shows the total surface area of predicted crystal habits in vacuum and solvents. The predicted crystal shape according to the AE model results with an aspect ratio of 5.12. The unique exhibiting facets contributions (%) are shown in **Fig. S1a**. The facet (002) is morphologically the most important whose percentage area is about 59.27%. The (100) facet has 14.32% area to be the second large surface. The (012), (10-2) and (110) facets have area 12.16%, 10.53% and 3.74%, respectively. The crystal habits generated from the AE model agrees with habit predictions published earlier. Controlling solvent evidently affects the crystal morphology of BA. The focus is now on the all visible total surface area of predicted crystal habit in solvent n-heptane. **Fig. S1b** shows no visibility of facet (100) and facet (012) covers a small part of the surface. The facet (10-2) covers the largest percentage of the surface. A lower share of the total surface area is contributed by the facet (002) and (110), respectively. The total surface area in solvent n-heptane is illustrated in **Fig. S1c**. The facet (10-2) is more extended and habit dominating. Facet (002) and (110) are visible, but

contributed only a small share to the total surface. Because of the relative larger polarity of n-heptane than n-hexane, the n-heptane molecule inhibits the growth of facet (10-2). In intermediate polarity solvents (Fig. S1d-f), similar morphologies shares of crystal habit surface coverage are reached. With the increase of solvent polarity, total surface area of predicted crystal habit in acetonitrile (Fig. S1g) shows different visible facets. The facet (012) with a lower share of the surface and facet (002) and (10-2) are dominating the habit.

#### 4. Experiments

A typical experimental procedure of the crystallization of BA in solvents can be found in our previous work<sup>3</sup>. BA was purchased from Sinopharm Chemical Regents Co., Ltd. Solvent n-hexane, n-heptane, acetone and acetonitrile were obtained from Beijing Chemical Works. All the reactants were of analytical reagent grade and used as received without any further purification. All glass wares (glass bottles and small pieces of glass substrates) were cleaned and then dried with oven. With the organic solvent volatilizing slowly at the room temperature, crystals were obtained. The morphologies of final BA crystals were observed with an optical microscope (Olympus BX-41, Japan).

#### 5. XRD characterization

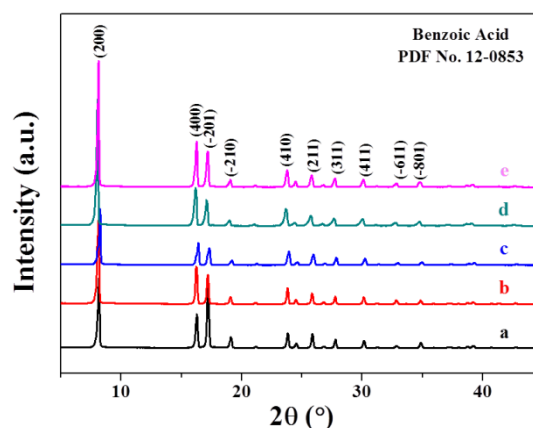


Fig. S2 Powder XRD patterns of products purchased (a) and recrystallized in solvents (b-n-hexane, c-n-heptane, d-acetone, e-acetonitrile)

Powder X-ray diffraction (XRD) measurements were performed on Bruker D8

Advance diffractometer with Cu K $\alpha$  radiation ( $\lambda = 1.54 \text{ \AA}$ ).

## 6. X-ray single crystal diffractometer results

The crystal structure of BA in solvent n-hexane was measured by X-ray single-crystal diffractometer (Agilent, Gemini E, America) with a Mo K $\alpha$  ( $\lambda = 0.7107 \text{ \AA}$ ) radiation in the range of 7.56 to 51.94 $^\circ$  ( $2\theta$ ) at 102.2 K. A total of 1984 diffraction points were collected and 1158 points were independent ( $R_{\text{int}} = 0.0160$ ). The crystal structure was solved by direct methods with the SHELXS-97 program and refined by a full-matrix least-square procedure based on  $F^2$ . The goodness-of-fit on  $F^2$ , the largest diffraction peak and hole were 1.051, 0.213 and  $-0.172\text{e\AA}^3$ , respectively. The final refinement continued until the final deviation factors,  $R_1$  and  $wR(F_2)$ , were 0.0466 and 0.0877. X-ray single crystal diffractometer result shows that the grown crystal belongs to the monoclinic system, space group  $P2_1/n$ , with the unit cell parameters  $a = 5.4253(7) \text{ \AA}$ ,  $b = 5.047(7) \text{ \AA}$ ,  $c = 21.698(3) \text{ \AA}$ ,  $\alpha = \gamma = 90.00^\circ$ ,  $\beta = 95.967(15)^\circ$ ,  $Z = 4$ ,  $F(000) = 256$ ,  $V = 591.0(9) \text{ \AA}^3$ , and  $D_c = 1.373 \text{ g/cm}^3$ , which was very agreement with the standard form mentioned in the reference.

**Table S2** Crystal structures of BA crystal from CSD (Cambridge Structural Database), measured, and reference results

Causes	CSD	Measured	Reference
Crystal system	monoclinic	monoclinic	monoclinic
Space group	$P2_1/c$	$P2_1/n$	$P2_1/c$
$a(\text{\AA})$	5.50	5.4253(7)	5.52(2)
$b(\text{\AA})$	5.128	5.047(7)	5.14(2)
$c(\text{\AA})$	21.950	21.698(3)	21.90(5)
$\alpha, \gamma(^\circ)$	90.00	90.00	90.00
$\beta(^\circ)$	97.370	95.967(15)	97.00
$Z$	4	4	4

The crystal structures of BA crystal in CSD, n-hexane, and reference paper were

shown in Table S2. The measured crystal structures proved that the form of crystal did not change.

Results of detail atomic coordinate, equivalent isotropic displacement parameter, bond lengths, bond angles, anisotropic displacement parameters and torsion angles are shown in Table S3-7.

**Table S3** Atomic coordinate and equivalent isotropic displacement parameter

<b>Atom</b>	<b>X/Å*10<sup>4</sup></b>	<b>Y/Å*10<sup>4</sup></b>	<b>Z/Å*10<sup>4</sup></b>	<b>U(eq)/Å<sup>2</sup>*10<sup>3</sup></b>
H2	1640	4666	380	36
H1	-1693	3866	-67	36
H2A	2515	731	1572	23
H4	-1566	-5103	2205	27
H3	1975	-2515	2301	27
H5	-4574	-4462	1380	29
H6	-4061	-1196	652	25
O2	1629.9	3556	655.5	23.8
C1	-722	102	1039.2	16.9
O1	-2036.7	2557	130.5	24
C2	1089	-304	1533.8	19.5
C4	-1352	-3800	1912.4	22.5
C3	768	-2251	1970	22.5
C5	-3158	-3413	1418.2	23.8
C6	-2849	-1460	981.7	20.7

\*U(eq) is defined as 1/3 of the trace of the orthogonalised  $U_{ij}$  tensor.

**Table S4** Bond lengths for BA crystal in n-hexane

<b>Atom</b>	<b>Atom</b>	<b>Length/Å</b>	<b>Atom</b>	<b>Atom</b>	<b>Length/Å</b>
O2	C7	1.2866(16)	C2	C3	1.388(2)
C1	C2	1.3927(19)	C4	C3	1.386(2)
C1	C6	1.393(2)	C4	C5	1.389(2)
C1	C7	1.487(2)	C5	C6	1.389(2)
O1	C7	1.2579(16)			

**Table S5** Bond angles for BA crystal in n-hexane

Atom	Atom	Atom	Angle/°	Atom	Atom	Atom	Angle/°
C2	C1	C6	119.82(13)	C4	C5	C6	120.06(13)
C2	C1	C7	120.10(12)	C5	C6	C1	119.88(13)
C6	C1	C7	120.08(13)	O2	C7	C1	116.62(12)
C3	C2	C1	120.08(13)	O1	C7	O2	123.80(13)
C3	C4	C5	120.14(14)	O1	C7	C1	119.57(12)
C4	C3	C2	120.02(13)				

**Table S6** Anisotropic displacement parameters ( $\text{\AA}^2 \cdot 10^3$ ) for BA crystal in n-hexane

Atom	U <sub>11</sub>	U <sub>22</sub>	U <sub>33</sub>	U <sub>23</sub>	U <sub>13</sub>	U <sub>17</sub>
O2	23.0(5)	24.3(6)	23.5(5)	2.8(4)	0.4(4)	-6.6(5)
C1	19.3(7)	16.1(7)	15.8(7)	-2.5(5)	4.0(5)	1.5(6)
O1	26.6(6)	24.0(6)	20.2(5)	3.4(4)	-3.1(4)	-2.5(5)
C2	19.3(7)	19.0(8)	20.3(7)	-2.3(6)	2.0(5)	-1.6(6)
C4	29.5(8)	17.1(8)	22.2(7)	2.3(6)	9.3(6)	2.1(6)
C3	25.9(8)	22.6(8)	18.5(7)	0.8(6)	-0.9(6)	2.5(6)
C5	20.8(7)	21.9(8)	29.4(8)	-0.9(6)	6.7(6)	-3.0(6)
C6	19.1(7)	21.5(8)	21.3(7)	-0.9(6)	0.7(5)	1.1(6)
C7	19.1(7)	18.1(8)	16.5(7)	-3.6(6)	2.4(5)	0.7(6)

**Table S7** Torsion angles for BA crystal in n-hexane

A	B	C	D	Angle/°
C1	C2	C3	C4	0.2(2)
C2	C1	C6	C5	0.1(2)
C2	C1	C7	O2	0.20(19)
C2	C1	C7	O1	-179.64(12)
C4	C5	C6	C1	0.2(2)
C3	C4	C5	C6	-0.3(2)
C5	C4	C3	C2	0.1(20)
C6	C1	C2	C3	-0.3(2)
C6	C1	C7	O2	-179.77(12)
C6	C1	C7	O1	0.4(2)
C7	C1	C2	C3	179.69(12)



**Supplementary references**

1. M. S. 6.0, Accelrys Software Inc., San Diego, CA, 2012.
2. C. Schmidt, C. Yürüdü, A. Wachsmuth and J. Ulrich, *CrystEngComm*, 2011, **13**, 1159-1169.
3. Q. H. Yi, J. F. Chen, Y. Le, J. X. Wang, C. Y. Xue and H. Zhao, *J. Cryst. Growth*, 2013, **372**, 193-198.